

**Georg-August-Universität
Göttingen**



**Inverse scattering for an impedance cylinder
buried in a dielectric cylinder**

**Rainer Kress, Fatih Yaman,
Ali Yapar, Ibrahim Akduman**

Nr. 2007-16

Inverse scattering for an impedance cylinder buried in a dielectric cylinder

Rainer Kress*, Fatih Yaman†, Ali Yapar† and Ibrahim Akduman†

October 15, 2007

Abstract

An inverse scattering problem is considered for arbitrarily shaped cylindrical objects that have inhomogeneous impedance boundaries and are buried in arbitrarily shaped cylindrical dielectrics. Given the shapes of the impedance object and the dielectric, the inverse problem consists of reconstructing the inhomogeneous boundary impedance from a measured far field pattern for an incident time-harmonic plane wave. Extending the approach suggested by Akduman and Kress [1] for an impedance cylinder in a homogeneous background medium, both the direct and the inverse scattering problem are solved via boundary integral equations. For the inverse problem, representing the scattered field as a potential leads to severely ill-posed linear integral equations of the first kind for the densities. For their stable numerical solution Tikhonov regularization is employed. Knowing the scattered field, the boundary impedance function can be obtained from the boundary condition either by direct evaluation or by a least squares approach. We provide a mathematical foundation of the inverse method and illustrate its feasibility by numerical examples.

1 Introduction

In electromagnetics, the impedance boundary condition is a tool for simplifying the solution of electromagnetic scattering problems involving complex structures. Commonly the boundary condition with a space dependent impedance coefficient is

*Institut für Numerische Angewandte Mathematik, Universität Göttingen, 37083 Göttingen, Germany

†Istanbul Technical University, Electrical and Electronics Engineering Faculty, 34469 Maslak, Istanbul, Turkey

used to model imperfectly conducting scatterers, perfectly conducting objects with a penetrable or absorbing boundary layer, or scatterers with a corrugated boundary. Its first application to a lossy material is generally attributed to Leontovich.

The determination of the boundary impedance for a given scatterer constitutes an important class of inverse scattering problems. In this paper we consider the scattering from an impedance object buried in a dielectric. This model corresponds to applications in biomedical imaging, nondestructive testing and geophysical explorations. In biomedical applications, for example, the bone of an arm can be modeled in terms of an inhomogeneous impedance boundary condition while the muscular structure over it can be considered as a lossy dielectric layer. In nondestructive evaluation of the coating on a conducting wire, the coating can be characterized as an arbitrarily shaped lossy dielectric layer and the conducting wire is modeled by an inhomogeneous surface impedance. The problem to determine the boundary impedance from scattering of time-harmonic waves by an impedance object with known shape that is buried in a dielectric is the topic of this paper. Motivated by the applications just mentioned, in a preliminary investigation we confine ourselves to a two-dimensional model case.

For the problem to recover the impedance function of an infinitely long cylindrical object with arbitrarily shaped cross section imbedded in a homogeneous background Akduman and Kress [1] suggested to use a boundary integral equation approach both for the corresponding direct and inverse problem. The aim of the present paper is to extend this approach to the case of an impedance cylinder buried in a cylindrical dielectric with arbitrary cross section.

To some extent, the inverse problem consists in solving a certain Cauchy problem, i.e., extending solutions to the Helmholtz equation from knowing their Cauchy data on some boundary curve. With this respect we also mention the related work of Jakubik and Potthast [6]. For the simultaneous reconstruction of the shape and the impedance in a homogeneous background we refer to Kress and Rundell [9] and to Serranho [11].

The plan of the paper is as follows. Since every investigation of inverse problems has to be based on a solid knowledge of the corresponding direct problem in Section 2 we give an existence analysis of the direct scattering problem based on boundary integral equations. This is followed by a short description of the numerical solution of the integral equations in Section 3. In the main Section 4 we present our inverse algorithm that again is based on boundary integral equations. In the final Section 5 some numerical examples exhibit the feasibility of our inverse method.

2 The direct problem

Consider a doubly connected bounded domain $D_0 \subset \mathbb{R}^2$ representing the cross section of an infinitely long homogeneous dielectric cylinder. We assume the boundary ∂D_0 to be C^2 smooth and denote the interior component of boundary curve by Γ_0 and the exterior component by Γ_1 , that is, $\partial D_0 = \Gamma_0 \cup \Gamma_1$ and $\Gamma_0 \cap \Gamma_1 = \emptyset$. We shall denote by ν_0 the unit normal to Γ_0 directed into the interior of D_0 and by ν_1 the unit normal to Γ_1 directed into the exterior of D_0 . The unbounded domain with boundary Γ_1 we denote by D_1 and consider it as the cross section of the homogeneous background medium.

Now, the direct scattering problem for a time-harmonic E -polarized electromagnetic wave with frequency ω subject to an impedance boundary condition is modeled by the following transmission boundary value problem for the Helmholtz equation. The total fields $u_0 \in C^2(D_0) \cap C^1(\overline{D_0})$ in D_0 and $u_1 \in C^2(D_1) \cap C^1(\overline{D_1})$ in D_1 representing the electric field parallel to the cylinder axis satisfy the Helmholtz equations

$$\Delta u_j + k_j^2 u_j = 0 \quad \text{in } D_j, \quad j = 0, 1, \quad (2.1)$$

with the wave numbers $k_j = \omega \sqrt{\mu_j (\varepsilon_j + i\sigma_j/\omega)}$ given in terms of the dielectric permittivity ε_j , the magnetic permeability μ_j , and the conductivity σ_j of the medium D_j . Note that the sign of the square root is chosen such that $\text{Re } k_j > 0$ and $\text{Im } k_j \geq 0$. In particular, throughout the paper, we shall assume that $\sigma_1 = 0$, i.e., k_1 is real and positive.

The total fields have to satisfy the *transmission conditions*

$$u_1 = u_0 \quad \text{and} \quad \frac{\partial u_1}{\partial \nu_1} = \frac{\partial u_0}{\partial \nu_1} \quad \text{on } \Gamma_1 \quad (2.2)$$

and the *impedance boundary condition*

$$u_0 + \frac{\eta}{ik_0} \frac{\partial u_0}{\partial \nu_0} = 0 \quad \text{on } \Gamma_0 \quad (2.3)$$

for some Hölder continuous function η satisfying

$$\text{Re} \frac{\eta}{k_0} \geq 0 \quad (2.4)$$

and

$$\eta(x) \neq 0 \quad (2.5)$$

for all $x \in \Gamma_0$. The condition (2.2) ensures the continuity of the tangential components of the electric and the magnetic field at the interface Γ_1 and the condition (2.3) model's the standard impedance condition on the boundary Γ_0 .

The external total field u_1 is decomposed $u_1 = u^i + u^s$ into the incident field u^i given by a plane wave $u^i = e^{ik_1 x \cdot d}$ where $d = (\cos \phi_0, \sin \phi_0)$ is the propagation direction with angle ϕ_0 and the scattered field u^s that has to satisfy the *Sommerfeld radiation condition*

$$\lim_{r \rightarrow \infty} \sqrt{r} \left(\frac{\partial u^s}{\partial r} - ik_1 u^s \right) = 0, \quad r = |x|, \quad (2.6)$$

uniformly for all directions. The Sommerfeld radiation condition (2.6) guarantees an asymptotic behavior of the scattered wave in the form of an outgoing wave

$$u^s(x) = \frac{e^{ik_1|x|}}{\sqrt{|x|}} \left\{ u_\infty \left(\frac{x}{|x|} \right) + O \left(\frac{1}{|x|} \right) \right\}, \quad |x| \rightarrow \infty, \quad (2.7)$$

uniformly for all directions with the amplitude factor u_∞ known as the far field pattern and defined on the unit circle Ω .

Theorem 2.1 *The direct scattering problem has at most one solution.*

Proof. Assume that u_1^1, u_0^1 and u_1^2, u_0^2 are two solutions to the direct scattering problem and consider the difference $u_1 := u_1^1 - u_1^2$ and $u_0 := u_0^1 - u_0^2$. Then u_1 and u_0 satisfy the Helmholtz equations (2.1), the boundary conditions (2.2) and (2.3) and in addition u_1 satisfies the radiation condition (2.6). Green's theorem, applied to u_0 in the domain D_0 yields

$$\int_{\Gamma_1} u_0 \frac{\partial \bar{u}_0}{\partial \nu_1} ds = \int_{\Gamma_0} u_0 \frac{\partial \bar{u}_0}{\partial \nu_0} ds + \int_{D_0} \{ |\text{grad} u_0|^2 - \bar{k}_0^2 |u_0|^2 \} dx. \quad (2.8)$$

From this, using the boundary conditions and taking the imaginary part, we obtain

$$\text{Im} \left(\int_{\Gamma_1} u_1 \frac{\partial \bar{u}_1}{\partial \nu_1} ds \right) = \int_{\Gamma_0} \text{Re} \left(\frac{\eta}{k_0} \right) \left| \frac{\partial \bar{u}_1}{\partial \nu_1} \right|^2 ds + \text{Im} (k_0^2) \int_{D_0} |u_0|^2 dx \geq 0,$$

provided the condition (2.4) is satisfied. Now, in view of the radiation condition for u_1 , from Theorem 2.12 in [3] we conclude that $u_1 = 0$ in D_1 . Finally Holmgren's uniqueness theorem (see Theorem 6.12 in [2]) and the transmission conditions (2.2) imply that $u_0 = 0$ in D_0 . \square

We establish existence of a solution to the direct scattering problem by adopting a potential approach to transform the scattering problem into a system of boundary integral equations. To this end, for $j = 0, 1$, we introduce the fundamental solutions Φ_j for the two-dimensional Helmholtz equation with wave number k_j by

$$\Phi_j(x, y) := \frac{i}{4} H_0^{(1)}(k_j |x - y|), \quad x \neq y,$$

in terms of the Hankel function $H_0^{(1)}$ of the first kind and order zero. Then, for $j, \ell, m = 0, 1$, we define single- and double-layer operators $S_{j\ell, m}$ and $K_{j\ell, m}$ by

$$(S_{j\ell, m}\varphi)(x) := 2 \int_{\Gamma_j} \Phi_m(x, y)\varphi(y) ds(y), \quad x \in \Gamma_\ell, \quad (2.9)$$

and

$$(K_{j\ell, m}\varphi)(x) := 2 \int_{\Gamma_j} \frac{\partial\Phi_m(x, y)}{\partial\nu_j(y)} \varphi(y) ds(y), \quad x \in \Gamma_\ell, \quad (2.10)$$

and the corresponding normal derivative operators $K'_{j\ell, m}$ and $T_{j\ell, m}$ by

$$(K'_{j\ell, m}\varphi)(x) := 2 \int_{\Gamma_j} \frac{\partial\Phi_m(x, y)}{\partial\nu_\ell(x)} \varphi(y) ds(y), \quad x \in \Gamma_\ell, \quad (2.11)$$

and

$$(T_{j\ell, m}\varphi)(x) := 2 \frac{\partial}{\partial\nu_\ell(x)} \int_{\Gamma_j} \frac{\partial\Phi_m(x, y)}{\partial\nu_j(y)} \varphi(y) ds(y), \quad x \in \Gamma_\ell. \quad (2.12)$$

The operators $S_{j\ell, m}, K_{j\ell, m}, K'_{j\ell, m} : C(\Gamma_j) \rightarrow C(\Gamma_\ell)$ are compact since they represent integral operators with weakly singular kernels for $j = \ell$ and continuous kernels for $j \neq \ell$. For $j \neq \ell$ the operator $T_{j\ell, m} : C(\Gamma_j) \rightarrow C(\Gamma_\ell)$ also has a continuous kernel and therefore is compact, but the operator $T_{jj, m}$ is a hypersingular operator that is only defined on subspaces $V_j \subset C(\Gamma_j)$ of sufficiently smooth functions. However, the difference operator $T_{jj, 1} - T_{jj, 0} : C(\Gamma_j) \rightarrow C(\Gamma_j)$ again has a weakly singular kernel and is compact. For these compactness properties we refer to Section 3.1 in [3].

In order to prove solvability of the direct scattering problem we seek the solution in the form of a combination of double- and single-layer potentials

$$u^s(x) = \int_{\Gamma_1} \left\{ \frac{\partial\Phi_1(x, y)}{\partial\nu_1(y)} \psi(y) + \Phi_1(x, y)\varphi(y) \right\} ds(y), \quad x \in D_1, \quad (2.13)$$

and

$$\begin{aligned} u_0(x) = & \int_{\Gamma_1} \left\{ \frac{\partial\Phi_0(x, y)}{\partial\nu_1(y)} \psi(y) + \Phi_0(x, y)\varphi(y) \right\} ds(y) \\ & + \int_{\Gamma_0} \Phi_0(x, y)\chi(y) ds(y), \quad x \in D_0. \end{aligned} \quad (2.14)$$

Then we can state the following theorem.

Theorem 2.2 *The fields given by (2.13) and (2.14) solve the direct scattering problem if the continuous densities ψ, φ and χ satisfy the system of integral equations*

$$\begin{aligned} 2\psi + K_{11,1}\psi - K_{11,0}\psi + S_{11,1}\varphi - S_{11,0}\varphi - S_{01,0}\chi &= -2u^i, \\ 2\varphi - T_{11,1}\psi + T_{11,0}\psi - K'_{11,1}\varphi + K'_{11,0}\varphi + K'_{01,0}\chi &= 2 \frac{\partial u^i}{\partial \nu_1}, \end{aligned} \quad (2.15)$$

$$\chi - (T_{10,0}\psi + K'_{10,0}\varphi + K'_{00,0}\chi) - \frac{ik_0}{\eta} (K_{10,0}\psi + S_{10,0}\varphi + S_{00,0}\chi) = 0.$$

Proof. We only sketch the proof. Clearly $u_1 = u^i + u^s$ and u_0 defined by (2.13) and (2.14) satisfy the Helmholtz equations (2.1) and additionally u^s satisfies the radiation condition. The mapping properties of the operators between Hölder spaces as described in Theorem 3.4 of [3] can be employed to show that for any continuous solution of the system (2.15) the density ψ is Hölder continuously differentiable and the densities φ and χ are Hölder continuous. This implies that u^s and u_0 have the required regularity $u_0 \in C^2(D_0) \cap C^1(\overline{D}_0)$ and $u^s \in C^2(D_1) \cap C^1(\overline{D}_1)$ and that the jump relations can be applied (see Theorem 3.3 in [3]). In particular, for the Hölder continuously differentiable density ψ the hypersingular operators $T_{11,m}$ can be applied. From the jump relations we then obtain

$$\begin{aligned} 2(u^s - u_0) &= K_{11,1}\psi + \psi + S_{11,1}\varphi - K_{11,0}\psi + \psi - S_{11,0}\varphi - S_{01,0}\chi, \\ 2\left(\frac{\partial u^s}{\partial \nu_1} - \frac{\partial u_0}{\partial \nu_1}\right) &= T_{11,1}\psi + K'_{11,1}\varphi - \varphi - T_{11,0}\psi - K'_{11,0}\varphi - \varphi - K'_{01,0}\chi, \\ 2\left(u_0 + \frac{\eta}{ik_0} \frac{\partial u_0}{\partial \nu_0}\right) &= K_{10,0}\psi + S_{10,0}\varphi + S_{00,0}\chi + \frac{\eta}{ik_0} (T_{10,0}\psi + K'_{10,0}\varphi + K'_{00,0}\chi - \chi). \end{aligned}$$

Therefore the system (2.15) implies that u_1 and u_0 satisfy the transmission and boundary conditions (2.2) and (2.3). \square

We introduce an operator $A : C(\Gamma_1) \times C(\Gamma_1) \times C(\Gamma_0) \rightarrow C(\Gamma_1) \times C(\Gamma_1) \times C(\Gamma_0)$ by

$$A := \begin{pmatrix} K_{11,1} - K_{11,0} & S_{11,1} - S_{11,0} & -S_{01,0} \\ -T_{11,1} + T_{11,0} & -K'_{11,1} + K'_{11,0} & K'_{01,0} \\ -2T_{10,0} - \frac{2ik_0}{\eta} K_{10,0} & -2K'_{10,0} - \frac{2ik_0}{\eta} S_{10,0} & -2K'_{00,0} - \frac{2ik_0}{\eta} S_{00,0} \end{pmatrix}$$

which obviously is compact since all its components are compact. Now, the system can be rewritten in the abbreviated form

$$(2I + A) \begin{pmatrix} \psi \\ \varphi \\ \chi \end{pmatrix} = 2 \begin{pmatrix} -u^i \\ \partial u^i / \partial \nu_1 \\ 0 \end{pmatrix}$$

where I is the identity operator.

Theorem 2.3 *The direct scattering problem has a unique solution, provided k_0^2 is not a Dirichlet eigenvalue of the negative Laplacian in the interior of Γ_0 .*

Proof. It suffices to prove that under the assumption on k_0 the system of integral equations (2.15) has a unique solution. To this end we show that the operator $2I + A$ is injective. Then the statement follows from the Riesz–Fredholm theory for compact operators. Assume that the densities ψ, φ and χ solve the homogeneous form of (2.15). Then the potentials in (2.13) and (2.14) solve the homogeneous transmission impedance problem. Therefore by the Theorem 2.1 we have $u_s = 0$ in D_1 and $u_0 = 0$ in D_0 . Since u_0 is continuous across Γ_0 the assumption on k_0 implies that $u_0 = 0$ in the interior of Γ_0 . Therefore the jump relations yield

$$\chi = \frac{\partial u_0^-}{\partial \nu_0} - \frac{\partial u_0^+}{\partial \nu_0} = 0 \quad \text{on } \Gamma_0.$$

Then the remaining densities ψ and φ solve

$$2 \begin{pmatrix} \psi \\ \varphi \end{pmatrix} + \begin{pmatrix} K_{11,1} - K_{11,0} & S_{11,1} - S_{11,0} \\ -T_{11,1} + T_{11,0} & -K'_{11,1} + K'_{11,0} \end{pmatrix} \begin{pmatrix} \psi \\ \varphi \end{pmatrix} = 0$$

and from Theorem 3.41 in [2] we can conclude that $\psi = \varphi = 0$. \square

We refrain from elaborating on how to avoid the assumption on k_0^2 not to be an interior Dirichlet eigenvalue by replacing the single-layer potential with density χ on Γ_0 by a combined single- and double-layer potential. We note that if we have absorption in D_0 , i.e., if $\sigma_0 > 0$ then the assumption on k_0 is always fulfilled.

3 Numerical solution of the direct problem

We assume that the boundary curves Γ_0 and Γ_1 are represented through regular parameterizations of the form

$$\Gamma_j = \{z_j(t) : t \in [0, 2\pi]\}, \quad j = 0, 1, \quad (3.1)$$

where $z_j : \mathbb{R} \rightarrow \mathbb{R}^2$ are 2π -periodic and twice continuously differentiable functions such that the orientation of Γ_j is counter-clockwise. Then the normal vectors are given by

$$\nu_j(t) = \frac{1}{|z'_j(t)|} [z'_j(t)]^\perp, \quad t \in [0, 2\pi], \quad (3.2)$$

where or any vector $a = (a_1, a_2)$, the vector $a^\perp := (a_2, -a_1)$ is obtained by rotating a clockwise by 90 degrees. Inserting (3.1) into the kernels of the integral operators we obtain for the single-layer operator

$$2\Phi_m(z_\ell(t), z_j(\tau)) = \frac{i}{2} H_0^{(1)}(k_m |z_\ell(t) - z_j(\tau)|)$$

and its normal derivative

$$2 \frac{\partial \Phi_m(z_\ell(t), z_j(\tau))}{\partial \nu(z_\ell(t))} = \frac{ik_m}{2} \frac{[z'_\ell(t)]^\perp \cdot [z_\ell(t) - z_j(\tau)]}{|z'_\ell(t)| |z_\ell(t) - z_j(\tau)|} H_0^{(1)'}(k_m |z_\ell(t) - z_j(\tau)|).$$

Analogously, we have the parameterized kernels of the double-layer operator

$$2 \frac{\partial \Phi_m(z_\ell(t), z_j(\tau))}{\partial \nu(z_j(\tau))} = \frac{ik_m}{2} \frac{[z'_j(\tau)]^\perp \cdot [z_j(\tau) - z_\ell(t)]}{|z'_j(\tau)| |z_\ell(t) - z_j(\tau)|} H_0^{(1)'}(k_m |z_\ell(t) - z_j(\tau)|)$$

and its normal derivative

$$2 \frac{\partial}{\partial \nu(z_\ell(t))} \frac{\partial \Phi_m(z_\ell(t), z_j(\tau))}{\partial \nu(z_j(\tau))} = U_{j\ell}(t, \tau) H_0^{(1)'}(k_m |z_\ell(t) - z_j(\tau)|) \\ + V_{j\ell}(t, \tau) \left\{ k_m H_0^{(1)''}(k_m |z_\ell(t) - z_j(\tau)|) - \frac{H_0^{(1)'}(k_m |z_\ell(t) - z_j(\tau)|)}{|z_\ell(t) - z_j(\tau)|} \right\}$$

where

$$U_{j\ell}(t, \tau) := -\frac{ik_m}{2} \frac{z'_\ell(t) \cdot z'_j(\tau)}{|z'_\ell(t)| |z'_j(\tau)| |z_\ell(t) - z_j(\tau)|}$$

and

$$V_{j\ell}(t, \tau) := \frac{ik_m}{2} \frac{[z'_\ell(t)]^\perp \cdot [z_\ell(t) - z_j(\tau)]}{|z'_\ell(t)| |z_\ell(t) - z_j(\tau)|} \frac{[z'_j(\tau)]^\perp \cdot [z_j(\tau) - z_\ell(t)]}{|z'_j(\tau)| |z_\ell(t) - z_j(\tau)|}$$

From this it can be seen that all the operators entering into the operator A have parameterized versions of the form

$$(M\varphi)(t) := \int_0^{2\pi} m(t, \tau) \varphi(\tau) d\tau, \quad t \in [0, 2\pi],$$

of an integral operator $M : C[0, 2\pi] \rightarrow C[0, 2\pi]$ mapping the space of continuous 2π periodic functions into itself. From the explicit expression for the Hankel functions in terms of Bessel and Neumann functions it follows that the kernels can be decomposed

$$m(t, \tau) = m_1(t, \tau) \ln \left(\sin^2 \frac{t - \tau}{2} \right) + m_2(t, \tau)$$

with smooth functions m_1 and m_2 . For details we refer to Section 3.5 of [3] and [7]. For integral equation system with this type of singular kernels, the Nyström method with quadrature rules based on trigonometric interpolation as described in Section 3.5 of [3] is at our disposal. We refrain from repeating the details. For a related error analysis we refer to [8] and note that we have exponential convergence for smooth, that is analytic boundary curves and impedance functions. The following examples exhibit this fast convergence for various types of non-convex boundaries with the parametric representation of the curves given in Table 3.1.

Contour Type	Parametric Representation
Apple Shaped:	$\Gamma^{(a)} = \left\{ \frac{0.5 + 0.4 \cos t + 0.1 \sin 2t}{1 + 0.7 \cos t} (\cos t, \sin t) : t \in [0, 2\pi] \right\}$
Circle:	$\Gamma^{(c)} = \{c_0(\cos t, \sin t) : t \in [0, 2\pi]\}$, c_0 : constant
Drop Shaped:	$\Gamma^{(d)} = \left\{ \left(-0.5 + 0.75 \sin \frac{t}{2}, -0.75 \sin t \right) : t \in [0, 2\pi] \right\}$
Ellipse:	$\Gamma^{(e)} = \{(e_0 \cos t, e_1 \sin t) : t \in [0, 2\pi]\}$, e_0, e_1 : constant
Kite Shaped:	$\Gamma^{(k)} = \{(\cos t + 1.3 \cos^2 t - 0.8, 1.5 \sin t) : t \in [0, 2\pi]\}$
Peanut Shaped:	$\Gamma^{(p)} = \left\{ \sqrt{\cos^2 t + 0.25 \sin^2 t} (\cos t, \sin t) : t \in [0, 2\pi] \right\}$
Rounded Triangle:	$\Gamma^{(r)} = \{(2 + 0.3 \cos 3t) (\cos t, \sin t) : t \in [0, 2\pi]\}$

Table 3.1: Parametric Representation of Boundary Curves

By the asymptotics of the Hankel function, the parametric representation of the far field pattern of the combined double- and single-layer potential (2.13) is given by

$$u_\infty(\hat{x}) = \gamma \int_0^{2\pi} \{k_1 [z_1'(\tau)]^\perp \cdot \hat{x} \psi(z_1(\tau)) + i \varphi(z_1(\tau)) |z_1'(\tau)|\} e^{-ik_1 z_1(\tau) \cdot \hat{x}} d\tau \quad (3.3)$$

where $\gamma = e^{-i\pi/4}/\sqrt{8\pi k_1}$ and $\hat{x} \in \Omega$. Table 3.2 gives some approximate values for the far field pattern $u_\infty(d)$ and $u_\infty(-d)$ in the forward direction d and the backscattering direction $-d$ obtained through evaluating (3.3) by the trapezoidal rule for the solution to the system of integral equations (2.15). The number of quadrature points in the Nyström method is $2n$. The direction d of the incident wave is $d = (1, 0)$. The impedance functions for the first and second example are

$$\eta_1(z_0(t)) = \sin^2 t + i \cos^2 t \quad \text{and} \quad \eta_2(z_0(t)) = e^{-(t-\pi)^2} + i \frac{\sin t}{100}.$$

Parameters:	n	$\text{Re } u_\infty(d)$	$\text{Im } u_\infty(d)$	$\text{Re } u_\infty(-d)$	$\text{Im } u_\infty(-d)$
$\Gamma_0 = \Gamma^{(p)}, \Gamma_1 = \Gamma^{(r)}$ $\eta = \eta_1$ $k_0 = 1, k_1 = 0.5$	8	0.76469029	0.33025282	-1.83100457	0.96201264
	16	0.76060633	0.34007177	-1.82590173	0.95574934
	32	0.76059742	0.34007960	-1.82589332	0.95574400
	64	0.76059742	0.34007960	-1.82589332	0.95574400
$\Gamma_0 = \Gamma^{(c)}, \Gamma_1 = \Gamma^{(e)}$ $c_0 = 1, e_0 = 3, e_1 = 2$ $\eta = \eta_2$ $k_0 = 2, k_1 = 0.25$	8	-0.74988421	1.20005719	-2.06346703	0.43885428
	16	-0.74916948	1.19966827	-2.06251065	0.43973667
	32	-0.74916933	1.19966791	-2.06251067	0.43973683
	64	-0.74916930	1.19966781	-2.06251067	0.43973686
$\Gamma_0 = \Gamma^{(e)}, \Gamma_1 = \Gamma^{(a)}$ $e_0 = 1.2, e_1 = 0.8$ $\eta = 0.2 - i0.3$ $k_0 = 3, k_1 = 2$	8	0.02828285	0.21769004	0.13572374	0.46599794
	16	0.01777448	0.23601195	0.13005604	0.48467119
	32	0.01776323	0.23596266	0.13009672	0.48461955
	64	0.01776322	0.23596267	0.13009673	0.48461956
$\Gamma_0 = \Gamma^{(k)}, \Gamma_1 = \Gamma^{(c)}$ $c_0 = 3$ $\eta = 1$ $k_0 = 4, k_1 = 1$	8	-0.89788315	-0.26054746	-2.74987888	1.53351515
	16	-0.70664878	-0.28046829	-2.68668081	1.50093930
	32	-0.70661800	-0.28043077	-2.68620811	1.50115647
	64	-0.70661800	-0.28043077	-2.68620811	1.50115647

Table 3.2: Numerical results for direct scattering problem

We used the following tests for the accuracy of our forward code. One can consider the transmission boundary value problem as treated in Chapter 3.8 of [2] as a special case of the direct problem presented in this paper for the case where

the impedance cylinder is omitted. Hence, first of all we compared our results with some results obtained by the method of moments for the transmission problem (see [4, 10]). For the two different methods we obtained the same results. However, we observed that for higher frequencies our Nyström method is much faster than the method of moments. Additionally, we considered the forward problem as presented in [1] as another special case of our direct problem when $k_0 = k_1 = 1$. Then, we compared the results with [1] and observed that they match accurately.

4 The inverse problem

As one of the most important tools in scattering theory, Rellich's lemma (see Theorem 2.13 in [3]) provides a one-to-one correspondence between radiating solutions to the Helmholtz equation and their far field pattern in the sense that $u_\infty = 0$ on Ω (or on an open subset of Ω) implies that $u^s = 0$ in D_1 .

The *inverse scattering problem* that we are concerned with is, given the shape of the scatterers, to determine the impedance function η from a knowledge of the far field pattern for one incident wave. We note that this inverse problem is nonlinear in the sense that the scattered wave depends nonlinearly on the impedance η as is obvious from the representation of the solution in Section 2. More importantly, the inverse problem is ill-posed since the determination of η does not depend continuously on the far field pattern in any reasonable norm. We will handle this issue of ill-posedness by using Tikhonov regularization.

However, concerning identifiability we first note that the far field pattern for one incident plane wave uniquely determines the impedance function η . As a consequence of Rellich's lemma the far field pattern uniquely determines u_1 in D_1 . Then, by Holmgren's theorem and the transmission conditions (2.2) the field u_0 is also uniquely determined in D_0 . From the impedance condition (2.3) we now can read off the uniqueness of η . Note that due to Holmgren's theorem the normal derivative of u_0 cannot vanish on open subsets of Γ_0 . Otherwise we first would conclude $u_0 = 0$ in D_0 and consequently $u_1 = 0$ in D_1 via the transmission conditions. This finally would lead to the contradiction that the incident plane wave would satisfy the radiation condition.

For our actual reconstruction algorithm we proceed along the proof of the above uniqueness result. From the given far field pattern we first reconstruct u^s in D_1 by seeking it in the form of a single-layer potential

$$u^s(x) = \int_{\Gamma_1} \Phi_1(x, y) \varphi(y) ds(y), \quad x \in D_1, \quad (4.1)$$

with unknown density $\varphi \in L^2(\Gamma_1)$. The single layer potential (4.1) has far field

pattern

$$u_\infty(\hat{x}) = \gamma \int_{\Gamma_1} e^{-ik_1 \hat{x} \cdot y} \varphi(y) ds(y), \quad \hat{x} \in \Omega, \quad (4.2)$$

(see (3.3)). Therefore, given the far field pattern u_∞ , the density φ is found by solving the integral equation of the first kind

$$S_\infty \varphi = u_\infty \quad (4.3)$$

with the compact operator $S_\infty : L^2(\Gamma_1) \rightarrow L^2(\Omega)$ given by

$$S_\infty(\varphi)(\hat{x}) := \gamma \int_{\Gamma_1} e^{-ik_1 \hat{x} \cdot y} \varphi(y) ds(y), \quad \hat{x} \in \Omega. \quad (4.4)$$

Due to the analytic kernel of S_∞ , the integral equation (4.3) is severely ill-posed. For a stable numerical solution of (4.3) Tikhonov regularization can be applied, that is, the ill-posed equation (4.3) is replaced by

$$\alpha \varphi_\alpha + S_\infty^* S_\infty \varphi_\alpha = S_\infty^* u_\infty \quad (4.5)$$

with some positive regularization parameter α and the adjoint $S_\infty^* : L^2(\Omega) \rightarrow L^2(\Gamma_1)$ of S_∞ . For the applicability of the Tikhonov regularization the following theorem on S_∞ is essential. For its proof we refer to Theorem 5.17 in [3].

Theorem 4.1 *The far field integral operator $S_\infty : L^2(\Gamma_1) \rightarrow L^2(\Omega)$ defined by (4.4) is injective and has dense range provided k_1^2 is not a Dirichlet eigenvalue for the negative Laplacian in the interior of Γ_1 .*

Once we have determined φ , and consequently u_1 via (4.1), we seek u_0 as a single-layer potential

$$u_0(x) = \int_{\Gamma_1} \Phi_0(x, y) \psi(y) ds(y) + \int_{\Gamma_0} \Phi_0(x, y) \chi(y) ds(y), \quad x \in D_0. \quad (4.6)$$

Given u^s via (4.1), it is an immediate consequence of the jump relations that the field (4.6) satisfies the transmission conditions (2.2) provided the densities ψ and χ solve the system of integral equations

$$\begin{aligned} S_{11,0} \psi + S_{01,0} \chi &= 2u^i + S_{11,1} \varphi \\ K'_{11,0} \psi + \psi + K'_{01,0} \chi &= 2 \frac{\partial u^i}{\partial \nu_1} + K'_{11,1} \varphi - \varphi \end{aligned} \quad (4.7)$$

If k_1^2 is not a Dirichlet eigenvalue for the interior of Γ_1 , then the inverse operator $(I + K'_{11,0})^{-1} : L^2(\Gamma_1) \rightarrow L^2(\Gamma_1)$ exists (see Theorem 3.17 in [2]) and we can eliminate ψ from (4.7) to obtain

$$\tilde{B}\chi = f \tag{4.8}$$

with the compact operator $B : L^2(\Gamma_0) \rightarrow L^2(\Gamma_1)$ given by

$$\tilde{B} := S_{01,0} - S_{11,0}(I + K'_{11,0})^{-1}K'_{01,0}$$

and the right-hand side

$$f := 2u^i + S_{11,1}\varphi + S_{11,0}(I + K'_{11,0})^{-1} \left(2 \frac{\partial u^i}{\partial \nu_1} + K'_{11,1}\varphi - \varphi \right).$$

The compactness of \tilde{B} illustrates the ill-posedness of the system (4.7). Rather than regularizing the eliminated version (4.8), in order to avoid the elimination step, we applied Tikhonov regularization directly to the system (4.7). To this end we need the following theorem.

Theorem 4.2 *The operator $B : L^2(\Gamma_1) \times L^2(\Gamma_0) \rightarrow L^2(\Gamma_1) \times L^2(\Gamma_1)$ given by the operator matrix*

$$B := \begin{pmatrix} S_{11,0} & S_{01,0} \\ K'_{11,0} + I & K'_{01,0} \end{pmatrix}$$

is injective and has dense range provided k_0^2 is not a Dirichlet eigenvalue for the negative Laplacian in the interior of Γ_0 .

Proof. For a solution of the homogeneous equation

$$B \begin{pmatrix} \psi \\ \chi \end{pmatrix} = 0$$

we first note that from the second equation we can conclude that ψ is continuous. Then, by the jump relations, the field u_0 defined by (4.6) satisfies $u_0 = 0$ and $\partial u_0 / \partial \nu_1 = 0$ on Γ_1 . Holmgren's uniqueness theorem implies $u_0 = 0$ in D_0 . Since the single-layer potential with L^2 density u_0 is continuous across Γ_0 (see [5], p. 176) under the assumption on k_0 we have $u_0 = 0$ in the interior of Γ_0 . Since u_0 is also continuous across Γ_1 by the uniqueness for the exterior Dirichlet problem in D_1 we have $u_0 = 0$ in D_1 . Summarizing, we have shown that $u_0 = 0$ in all of \mathbb{R}^2 and the jump relations for L^2 densities (see pp. 45 in [3]) imply that $\psi = \chi = 0$.

To establish that B has dense range it suffices to show that its adjoint $B^* : L^2(\Gamma_1) \times L^2(\Gamma_1) \rightarrow L^2(\Gamma_1) \times L^2(\Gamma_0)$ as given by

$$B^* \begin{pmatrix} \psi \\ \chi \end{pmatrix} = \begin{pmatrix} \overline{S_{11,0}\psi} & \overline{K_{11,0}\chi} + \chi \\ \overline{S_{10,0}\psi} & \overline{K_{10,0}\chi} \end{pmatrix}$$

is injective. For a solution to the homogeneous equation

$$B^* \begin{pmatrix} \psi \\ \chi \end{pmatrix} = 0 \quad (4.9)$$

we define

$$v(x) = \int_{\Gamma_1} \Phi_0(x, y) \overline{\psi(y)} ds(y) + \int_{\Gamma_1} \frac{\partial \Phi_0(x, y)}{\partial \nu_1} \overline{\chi(y)} ds(y), \quad x \notin \Gamma_0.$$

Then the first equation of (4.9) implies that v solves the exterior Dirichlet problem in D_1 with homogeneous boundary condition $v = 0$ on Γ_1 and consequently $v = 0$ in D_1 . The second equation of (4.9) implies that v solves the Dirichlet problem in the interior of Γ_0 with homogeneous boundary condition $v = 0$ on Γ_0 . Hence, under the assumption on k_0 we also have $v = 0$ in the interior of Γ_0 and by analyticity this extends to $v = 0$ in the interior of Γ_1 . Again since $v = 0$ in all of \mathbb{R}^2 , the jump relations imply that $\psi = \chi = 0$. \square

We note that for the numerical approximation of the operator B we can make use of the same quadrature rules as mentioned in Section 3. Once we have determined ψ and χ through Tikhonov regularization of (4.7) we can compute

$$2u_0 = S_{10,0}\psi + S_{00,0}\chi \quad \text{and} \quad 2 \frac{\partial u_0}{\partial \nu_0} = K'_{10,0}\psi + K'_{00,0}\chi - \chi \quad \text{on } \Gamma_0. \quad (4.10)$$

Then, in principle, for each point $x \in \Gamma_0$ we finally can read off the impedance function from (2.3) as

$$\eta = - \frac{ik_0 u_0}{\frac{\partial u_0}{\partial \nu_0}} \quad \text{on } \Gamma_0. \quad (4.11)$$

However, the reconstruction of the impedance from the equation (4.11) will be sensitive to errors in the normal derivative of u_0 in the vicinity of zeros. To obtain more stable solutions, we express the unknown impedance function in terms of some basis functions γ_n , $n = 1, \dots, N$, as a linear combination

$$\eta = \sum_{n=1}^N c_n \gamma_n \quad \text{on } \Gamma_0. \quad (4.12)$$

A possible choice of basis functions consists of splines or trigonometric polynomials. Then we satisfy (2.3) in a least squares sense, that is, we determine the coefficients c_1, \dots, c_N in (4.12) such that for a set of grid points x_1, \dots, x_M on Γ_0 the least squares sum

$$\sum_{m=1}^M \left| u_0(x_m) + \frac{1}{ik_0} \sum_{n=1}^N c_n \gamma_n(x_m) \frac{\partial u_0}{\partial \nu_0}(x_m) \right|^2 \quad (4.13)$$

is minimized. The number of basis functions N in (4.12) can be considered as some kind of additional regularization parameter.

5 Numerical results

In this final section we present some numerical examples in order to show the effectiveness and the accuracy of the method described in the previous sections. In these examples all of the integral equation systems are solved through the Nyström method with a discretization number $n = 64$. The integral appearing in the far field expression (3.3) is evaluated numerically by using the trapezoidal rule. For the approximation of the impedance in (4.12) we used trigonometric polynomials of degree less than or equal to N . The Tikhonov regularization parameters for the equations (4.3) and (4.7) are denoted by α_1 and α_2 , respectively.

We choose various shaped, smooth impedance and dielectric cylinders given in Table 3.1, for various kinds of continuous impedance functions, for different wave numbers and different angles of incidence. For noisy data, random errors were added pointwise to the u_∞ with a noise level of 3%. In all examples the regularization parameters were chosen by trial and error.

In the first example, the shape of the impedance cylinder is chosen as a kite shaped scatterer $\Gamma_0 = \Gamma^{(k)}$ whereas the dielectric cylinder is a circular cylinder $\Gamma_1 = \Gamma^{(c)}$ with radius $c_0 = 2.5$. The impedance function over the boundary Γ_0 is given as

$$\eta(z_0(t)) = \sin^4 \frac{t}{2} + i \cos^4 \frac{t}{2}. \quad (5.1)$$

The wave numbers are chosen as $k_0 = 1$ and $k_1 = 0.5$ and the illumination angle is $\phi_0 = 180$ for both exact data and noisy data. For exact data, the Tikhonov parameters are $\alpha_1 = 10^{-8}$, $\alpha_2 = 5 \times 10^{-5}$, and for the noisy case, $\alpha_1 = 5 \times 10^{-3}$, $\alpha_2 = 10^{-2}$ is chosen. The degree of the polynomial is $N = 9$ and $N = 5$ for the exact and noisy case, respectively.

As a second example, two elliptical cylinders are chosen: $\Gamma_0 = \Gamma^{(e)}$ with semi-axis $e_0 = 1.5$, $e_1 = 1.2$ and $\Gamma_1 = \Gamma^{(e)}$ with semi-axis $e_0 = 2.5$, $e_1 = 2.2$. The incident

angle is $\phi_0 = 0$, the inhomogeneous surface impedance is

$$\eta(z_0(t)) = 1.5 + \sin^3 t + i \sin t \quad (5.2)$$

and the wave numbers are $k_0 = 2$ and $k_1 = 1.5$ for noisy and exact data. The parameters $\alpha_1 = \alpha_2 = 10^{-8}$, $N = 9$ are chosen for the noiseless case and $\alpha_1 = 3 \times 10^{-1}$ and $\alpha_2 = 5 \times 10^{-4}$, $N = 7$ for the noisy case.

In the third application, the impedance cylinder is considered as a drop shaped scatterer $\Gamma_0 = \Gamma^{(d)}$ and the dielectric cylinder is an elliptical cylinder $\Gamma_1 = \Gamma^{(e)}$ with semi-axis $e_0 = 1, e_1 = 1.5$. Both for the noiseless and noisy case, the incident angle is $\phi_0 = 180$, the wave numbers are $k_0 = 3$ and $k_1 = 2$. The inhomogeneous surface impedance is

$$\eta(z_0(t)) = 0.5e^{-(t-\pi)^2} + i(0.6 + 0.2 \sin t). \quad (5.3)$$

The parameters $\alpha_1 = 10^{-5}$, $\alpha_2 = 10^{-5}$, $N = 5$ are chosen for exact data and $\alpha_1 = 10^{-3}$ and $\alpha_2 = 8 \times 10^{-3}$, $N = 3$ for the noisy case.

In the final example, the impedance cylinder is considered as a peanut shaped $\Gamma_0 = \Gamma^{(p)}$ and the dielectric cylinder is a circle $\Gamma_1 = \Gamma^{(c)}$ with radius $c_0 = 1.5$. The incident angle is $\phi_0 = 0$ and the wave numbers are $k_0 = 1$ and $k_1 = 0.5$. The inhomogeneous surface impedance is

$$\eta(z_0(t)) = \frac{4 + \sin t}{5 + \cos t} + i \frac{\cos t}{7 - \sin t}. \quad (5.4)$$

The parameters are $\alpha_1 = 10^{-6}$, $\alpha_2 = 10^{-4}$, $N = 5$ for exact data and $\alpha_1 = 0.2$ and $\alpha_2 = 10^{-2}$, $N = 3$ for noisy data.

6 Conclusions

The applicability and the effectiveness of our method is supported by the numerical results. As to be expected, exact data yield slightly better reconstructions than noisy data and we observed that if the noise level exceeds 3%–4% then the reconstructions start to deteriorate. Additionally, for exact data we need smaller Tikhonov regularization parameters and can use higher degrees for the trigonometric polynomials, however for the noisy case we need stronger regularization parameters and a smaller degree of the polynomials. We also observed that in the noise free case we can reconstruct the impedance function satisfactorily. However, for noisy data small perturbations of the shape of the dielectric cylinder effects the success of the reconstruction significantly. On the other hand, the shape of the impedance cylinder does not effect the reconstructions as much as the shape of the dielectric cylinder. It is obvious that the illumination angle also effects the reconstructions depending

on the geometry of the scatterers. We expect that the method can be extended to a larger number of dielectric layers and, in principle, also to three-dimensional problems.

Acknowledgment. This research was carried out while Fatih Yaman was visiting the University of Göttingen as a fellow of the Deutsche Akademische Auslandsdienst (DAAD). The hospitality of the University of Göttingen and the support of the DAAD are gratefully acknowledged.

References

- [1] Akduman, I. and Kress R.: Direct and inverse scattering problems for inhomogeneous impedance cylinders of arbitrary shape. *Radio Sci.* **38**, 1055–1064 (2003).
- [2] Colton, D. and Kress, R.: *Integral Equation Methods in Scattering Theory*. Wiley-Interscience Publications, New York 1983.
- [3] Colton, D. and Kress, R.: *Inverse Acoustic and Electromagnetic Scattering Theory*. 2nd. ed. Springer Verlag, Berlin 1998.
- [4] Harrington, R.F.: Matrix methods for field problems. *Proceedings of the IEEE* **55**, 136–149 (1967).
- [5] Henrici, P.: *Applied and Computational Complex Analysis*, Vol 3. Wiley-Interscience Publications, New York 1986.
- [6] Jakubik, P. and Potthast, R.: Testing the integrity of some cavity - the Cauchy problem and the range test. *Applied Numerical Mathematics* (to appear).
- [7] Kress, R.: On the numerical solution of a hypersingular integral equation in scattering theory. *Journal of Computational and Applied Mathematics* **61**, 345–360 (1995).
- [8] Kress, R.: *Integral Equations*. 2nd. ed Springer Verlag, Berlin 1998.
- [9] Kress, R. and Rundell, W.: Inverse scattering for shape and impedance. *Inverse Problems* **17**, 1075–1085 (2001).
- [10] Richmond, J.H.: Scattering by a dielectric cylinder of arbitrary cross section shape. *IEEE Trans. Antennas and Propagation* **13**, 334–341 (1965).
- [11] Serranho, P.: A hybrid method for inverse scattering for shape and impedance. *Inverse Problems* **22**, 663–680 (2006).

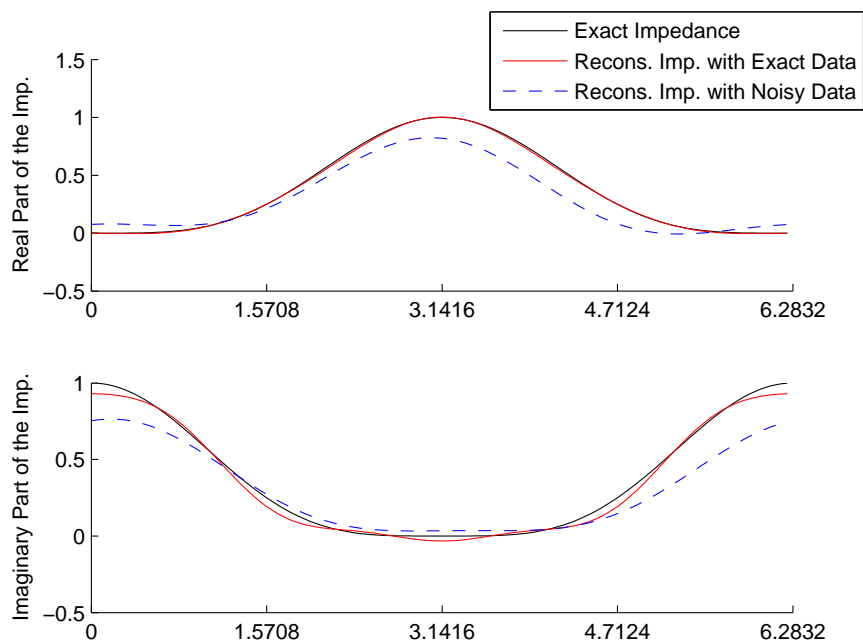


Figure 1: Reconstruction of the impedance (5.1) for a kite–circle geometry.

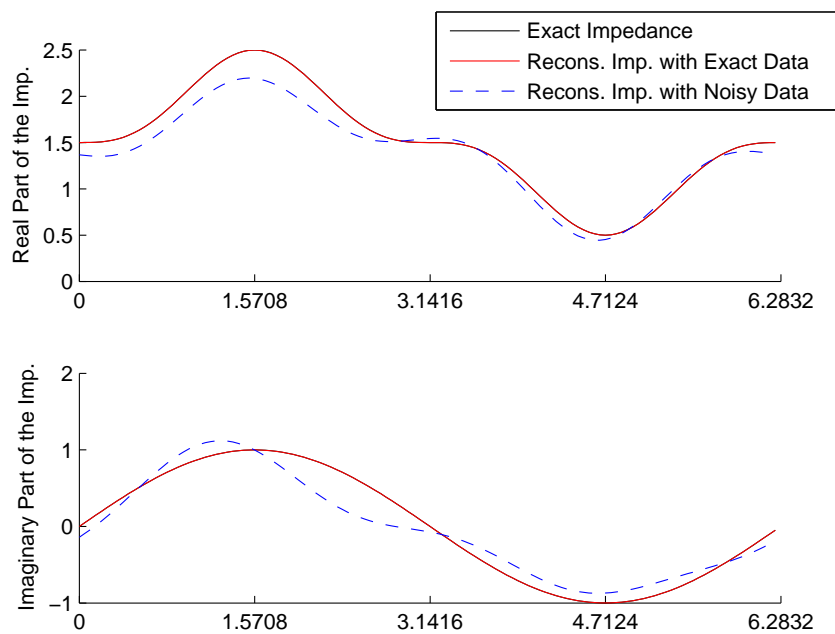


Figure 2: Reconstruction of the impedance (5.2) in an ellipse–ellipse geometry.

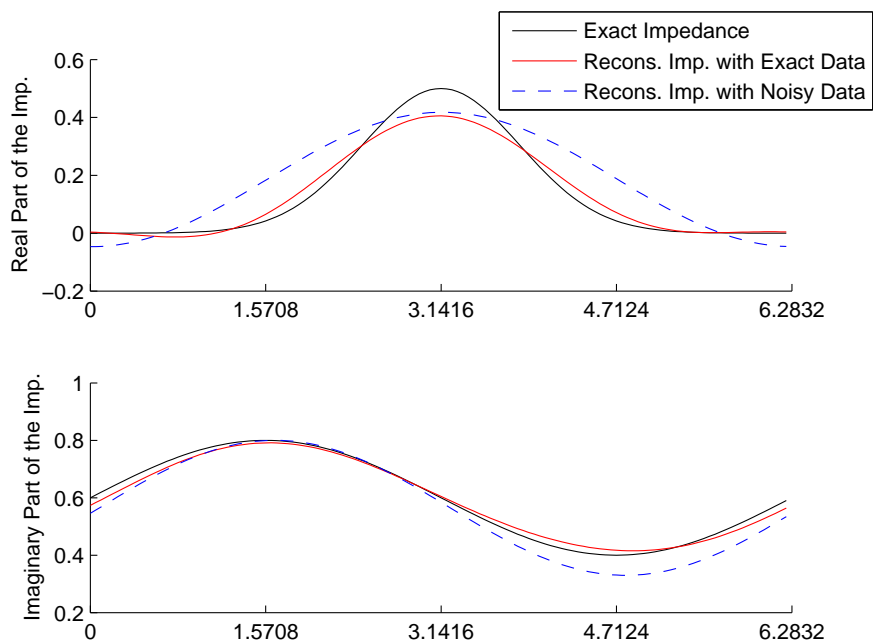


Figure 3: Reconstruction of the impedance (5.3) in a drop-ellipse geometry.

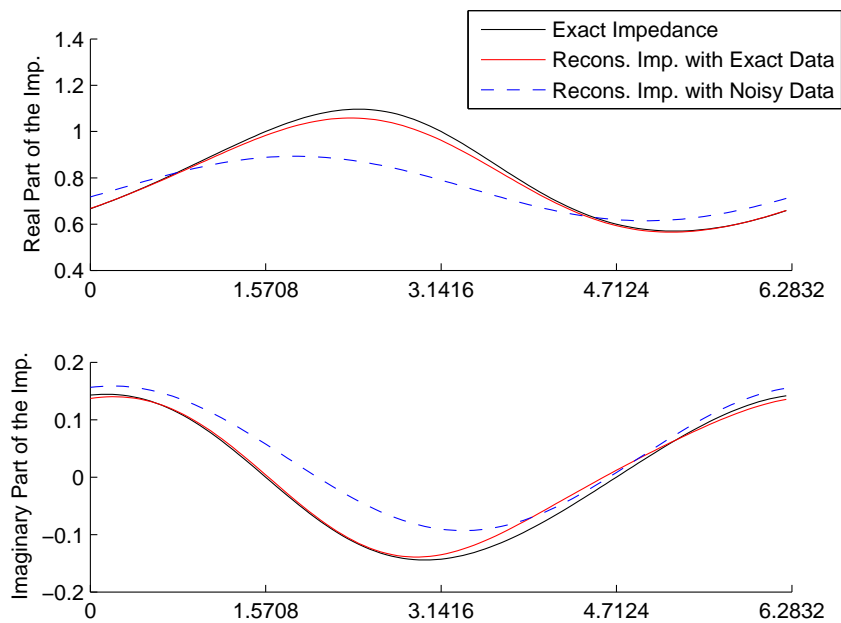


Figure 4: Reconstruction of the impedance (5.4) in a peanut-circle geometry.

Institut für Numerische und Angewandte Mathematik
Universität Göttingen
Lotzestr. 16-18
D - 37083 Göttingen

Telefon: 0551/394512

Telefax: 0551/393944

Email: trapp@math.uni-goettingen.de URL: <http://www.num.math.uni-goettingen.de>

Verzeichnis der erschienenen Preprints 2007:

- | | | |
|---------|--|---|
| 2007-01 | P. Serranho | A hybrid method for inverse scattering for sound-soft obstacles in 3D |
| 2007-02 | G. Matthies, G. Lube | On streamline-diffusion methods for inf-sup stable discretisations of the generalised Oseen Problem |
| 2007-03 | A. Schöbel | Capacity constraints in delay management |
| 2007-04 | J. Brimberg, H. Juel,
A. Schöbel | Locating a minisum circle on the plane |
| 2007-05 | C. Conte, A. Schöbel | Identifying dependencies among delays |
| 2007-06 | D.S. Gilliam, T. Hohage, X. Ji,
F. Ruymgaart | The Frechet-derivative of an analytic function of a bounded operator with some applications |
| 2007-07 | T. Hohage, M. Pricop | Nonlinear Tikhonov regularization in Hilbert scales for inverse boundary value problems with random noise |
| 2007-08 | C.J.S. Alves, R. Kress, A.L. Silvestre | Integral equations for an inverse boundary value problem for the two-dimensional Stokes equations |
| 2007-09 | A. Ginkel, A. Schöbel | To wait or not to wait? The bicriteria delay management problem in public transportation |
| 2007-10 | O. Ivanyshyn, R. Kress | Inverse scattering for planar cracks via nonlinear integral equations |
| 2007-11 | F. Delbary, K. Erhard,
R. Kress, R. Potthast, J. Schulz | Inverse electromagnetic scattering in a two-layered medium with an application to mine detection |
| 2007-12 | M. Pieper | Vector hyperinterpolation on the sphere |
| 2007-13 | M. Pieper | Nonlinear integral equations for an inverse electromagnetic scattering problem |
| 2007-14 | I. Akduman, R. Kress, N. Tezel,
F. Yaman | A second order Newton method for sound soft inverse obstacle scattering |

- 2007-15 M. Schachtebeck, A. Schöbel Algorithms for delay management with capacity constraints
- 2007-16 R. Kress, F. Yaman, A. Yapar, I. Akduman Inverse scattering for an impedance cylinder buried in a dielectric cylinder